Science Advances
AAAS

advances.sciencemag.org/cgi/content/full/6/40/eabb5223/DC1

Supplementary Materials for

Nanoscale metal-organic frameworks for x-ray activated in situ cancer vaccination

Kaiyuan Ni, Guangxu Lan, Nining Guo, August Culbert, Taokun Luo, Tong Wu, Ralph R. Weichselbaum, Wenbin Lin*

*Corresponding author. Email: wenbinlin@uchicago.edu

Published 2 October 2020, *Sci. Adv.* **6**, eabb5223 (2020)
DOI: 10.1126/sciadv.abb5223

This PDF file includes:

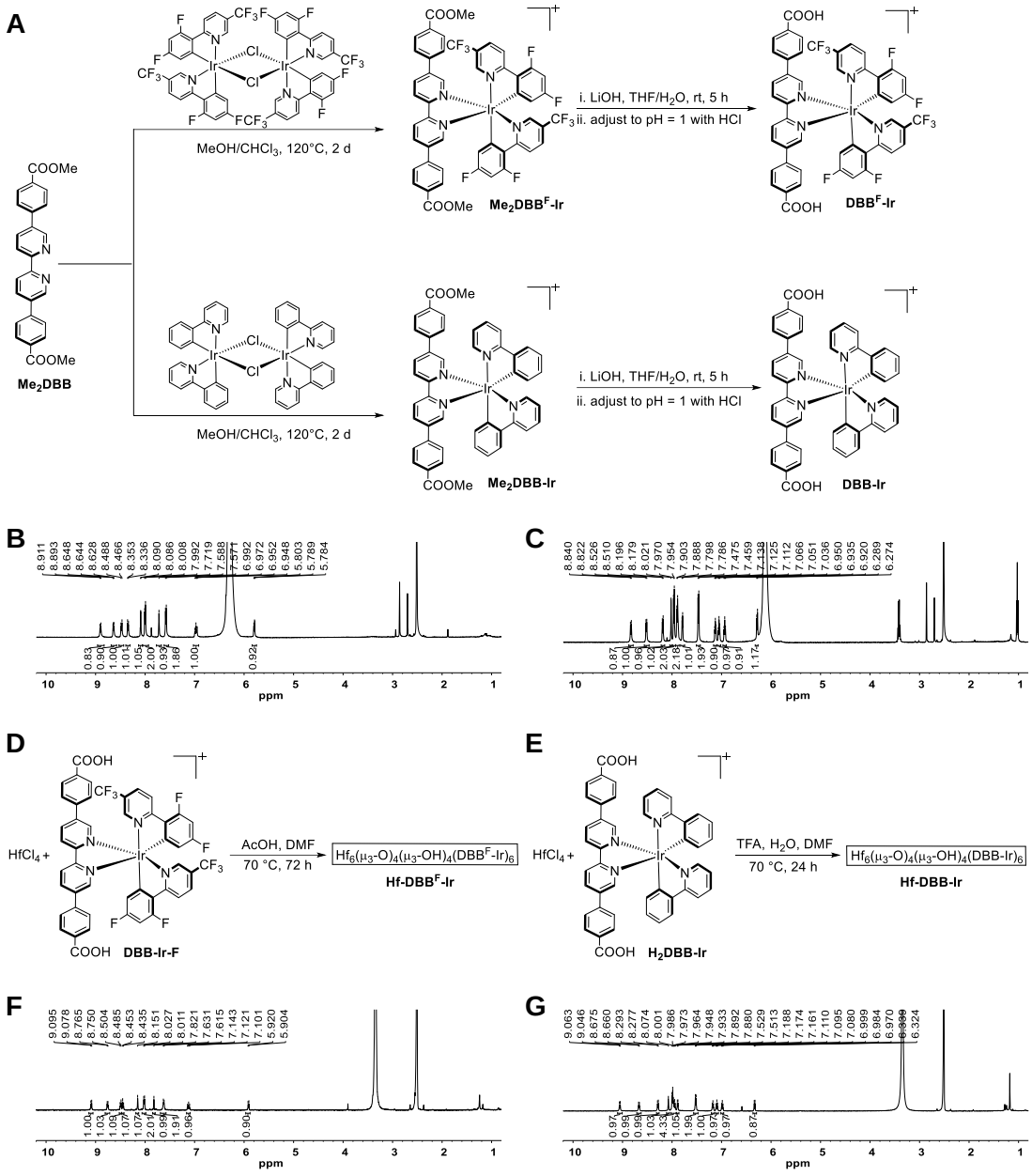

Fig. S1. Synthesis of DBB^F-Ir, DBB-Ir, Hf-DBB^F-Ir, and Hf-DBB-Ir. (**A**) Synthesis routes of DBB^F-Ir and DBB-Ir. ^{1}H NMR spectra of DBB^F-Ir (**B**) and DBB-Ir (**C**) in DMSO-d_6. Synthesis routes of Hf-DBB^F-Ir (**D**) and Hf-DBB-Ir (**E**). ^{1}H NMR spectra of digested Hf-DBB^F-Ir (**F**) and Hf-DBB-Ir (**G**) in DMSO-d_6.

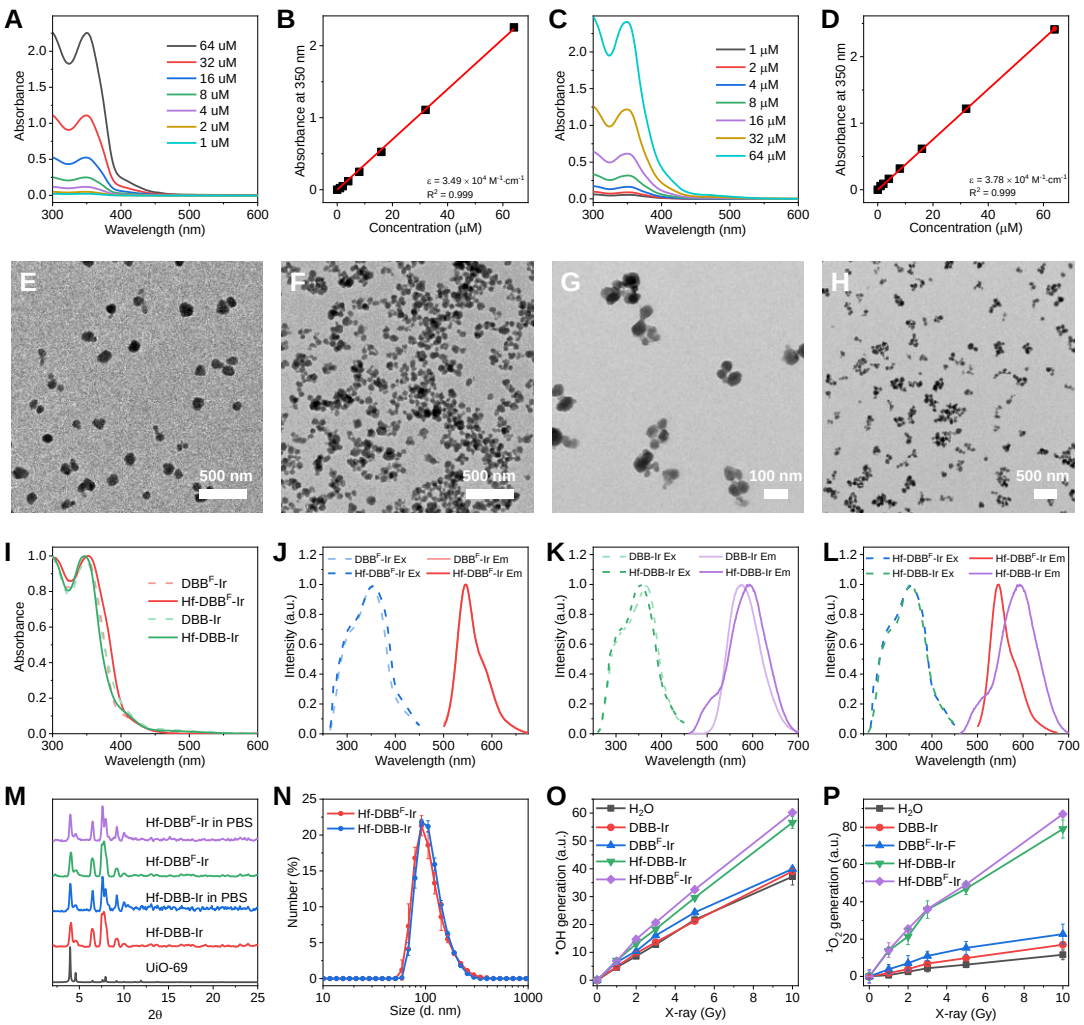

Fig. S2. Characterization of DBB^F-Ir, DBB-Ir, Hf-DBB^F-Ir, and Hf-DBB-Ir. UV-vis spectra of DBB^F-Ir (**A**) and its linear fit between the absorbance at 350 nm and the concentration (**B**). UV-vis spectra of DBB-Ir (**C**) and its linear fit between the absorbance at 350 nm and the concentration (**D**). The extinction coefficients (ε) of DBB^F-Ir and DBB-Ir were determined to be 3.49×10^4 $M^{-1}cm^{-1}$ and 3.78×10^4 $M^{-1}cm^{-1}$, respectively. Large-area TEM images of Hf-DBB^F-Ir (**E**) and Hf-DBB-Ir (**F**). (**G** & **H**) TEM images of Hf-DBB^F-Ir@CpG. (**I**) UV-vis spectra of Hf-DBB^F-Ir and Hf-DBB-Ir in comparison to those of DBB^F-Ir and DBB-Ir, respectively. Excitation and emission spectra of Hf-DBB^F-Ir (**J**) and Hf-DBB-Ir (**K**) in comparison to those of DBB^F-Ir and DBB-Ir, respectively. (**L**) Excitation and emission spectra of Hf-DBB^F-Ir and Hf-DBB-Ir. (**M**) PXRD patterns of Hf-DBB^F-Ir and Hf-DBB-Ir, freshly prepared or after 24 h incubation in 0.6 mM PBS, in comparison to that of UiO-69. (**N**) Number-averaged diameters of Hf-DBB^F-Ir (112.2 ± 2.8 nm) and Hf-DBB-Ir (113.9 ± 1.6 nm) in EtOH, n=3. (**O**) $^{\bullet}OH$ generation of H_2O, DBB-Ir, DBB^F-Ir, Hf-DBB-Ir, and Hf-DBB^F-Ir as determined by APF assay, n=3. (**P**) $^1O_2$ generation of H_2O, DBB-Ir, DBB^F-Ir, Hf-DBB-Ir, and Hf-DBB^F-Ir as determined by SOSG assay, n=3.

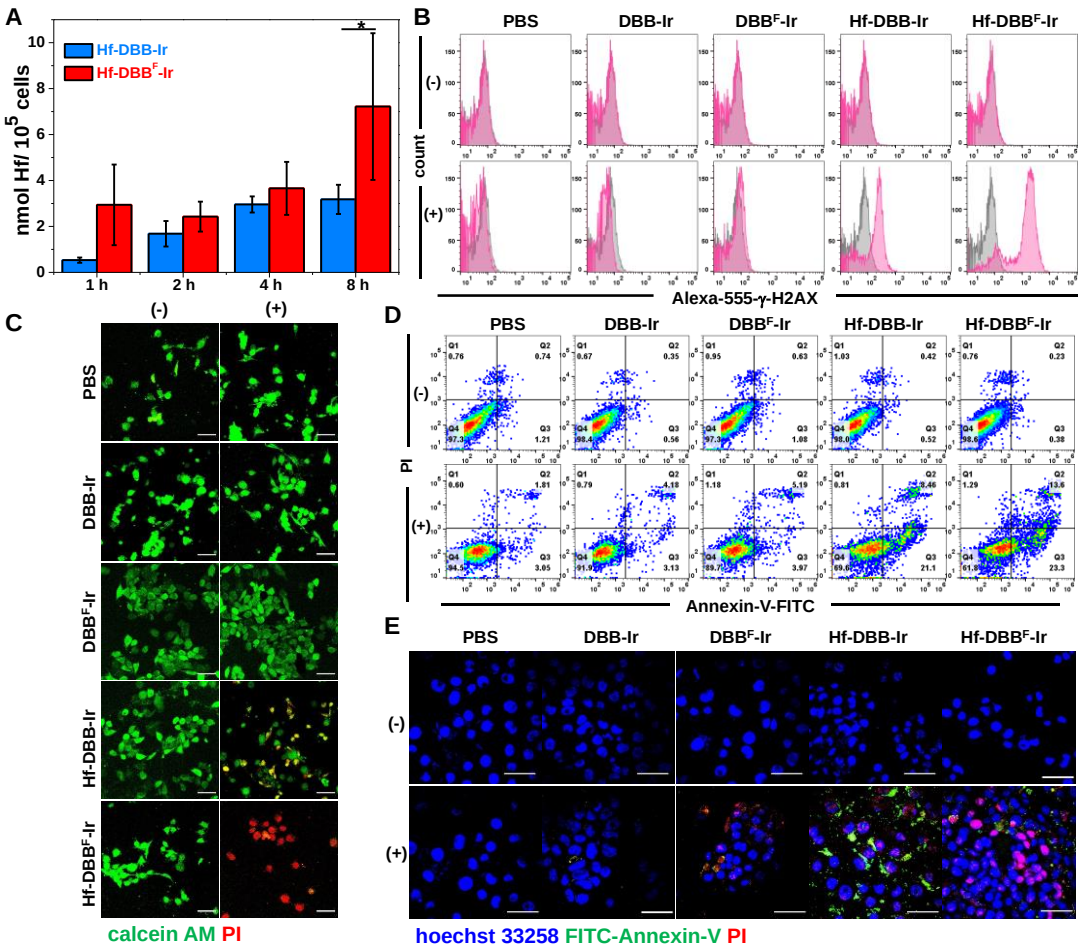

Fig. S3. ***In vitro*** **RT-RDT effect.** (**A**) Cellular uptake of Hf-DBB-Ir and Hf-DBB^{F}-Ir on MC38 cells after 1, 2, 4, or 8 hours of incubation with 20 μM Hf-DBB-Ir or Hf-DBB^{F}-Ir based on Hf, n=3. The Hf concentrations were determined by ICP-MS. MC38 cells were treated with PBS, DBB-Ir, DBB^{F}-Ir, Hf-DBB-Ir, or Hf-DBB^{F}-Ir for 4 h and then irradiated upon X-ray at a dose of 0 (-) or 2 (+) Gy for the following assays. (**B**) Flow cytometric analysis of DNA double strain breaks probed by γ-H2AX in treated MC38 cells. Grey histogram (control), and carmine histogram show the difference of γ-H2AX level in the cells, respectively. (**C**) Representative CLSM images of Live/dead cell analysis. Green and red fluorescence represent Calcein AM and PI signal, indicating live or dead cells, respectively. (**D**) Flow cytometric Annexin V/PI analysis with the quadrants from lower left to upper left (counter clockwise) represent healthy, early apoptotic, late apoptotic, and necrotic cells, respectively. The percentage of cells in each quadrant was shown on the graphs. (**E**) Representative CLSM images for apoptosis with Blue, red and green fluorescence representing DAPI, PI and Annexin-V-conjugated Alexa-488, respectively. Scale bar = 50 μm.

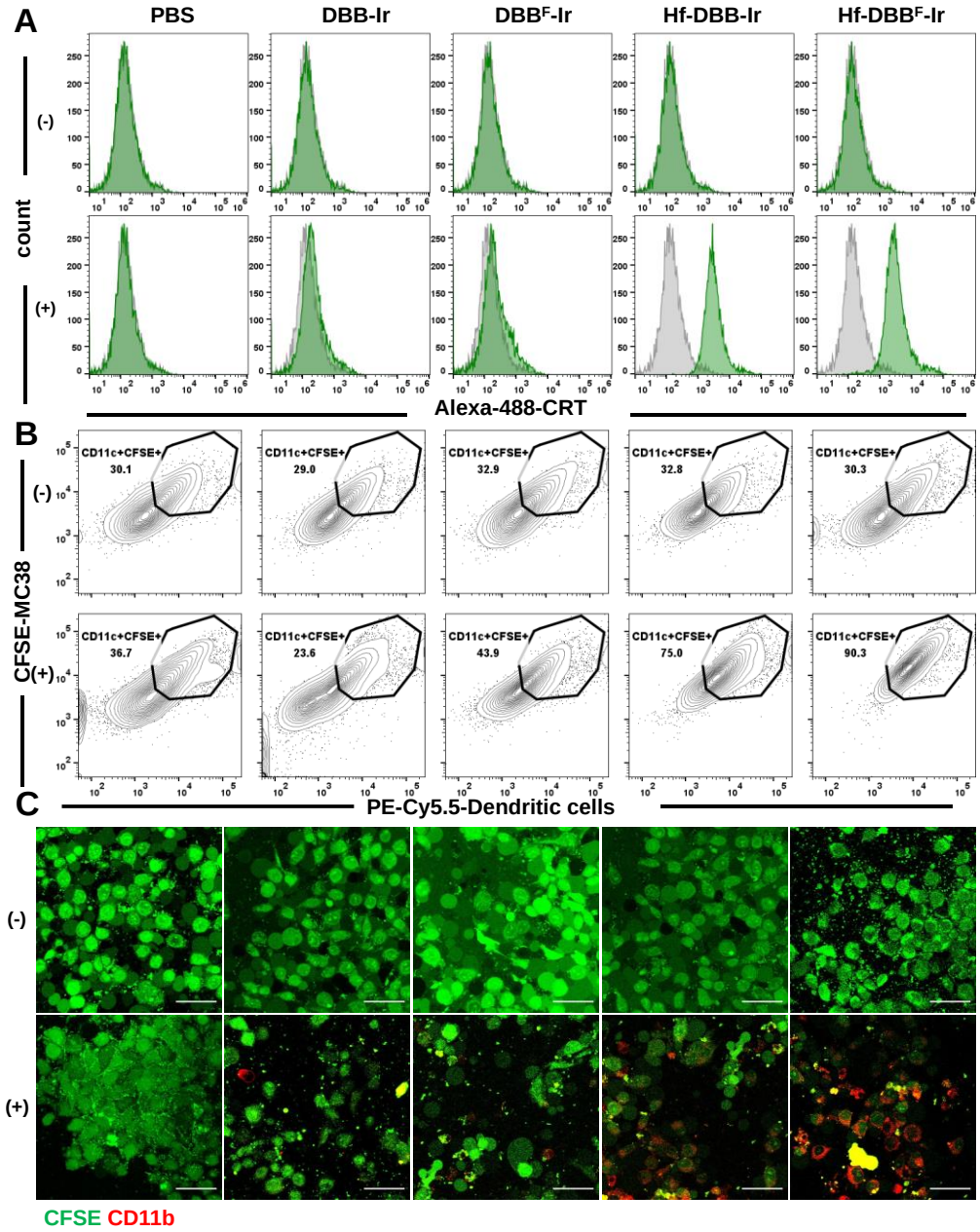

Fig. S4. Generation of DAMPs and phagocytosis. MC38 cells were treated with PBS, DBB-Ir, DBB^F-Ir, Hf-DBB-Ir, or Hf-DBB^F-Ir for 4 h and then irradiated upon X-ray at a dose of 0 (-) or 2 (+) Gy and co-cultured with DCs for phagocytosis assay. (**A**) Flow cytometric analysis of calreticulin exposure in treated MC38 cells. Grey histogram (control) and green histogram show the difference of CRT level in the cells, respectively. (**B**) Phagocytosis of CFSE-labelled MC38 cells by DCs analyzed by flow cytometry. DCs co-cultured with treated MC38 cells were stained with PE-Cy5.5-conjugated CD11c antibody. CD11c$^+$CFSE$^+$ double positive population was gated as DC-phagocytosed MC38 cells. (**C**) Representative CLSM images of phagocytosis of MC38 cells by DCs. Green and red fluorescence represent CFSE-labelled MC38 cells and PE-Cy5.5-conjugated CD11c labelled DCs, respectively. Scale bar = 50 μm.

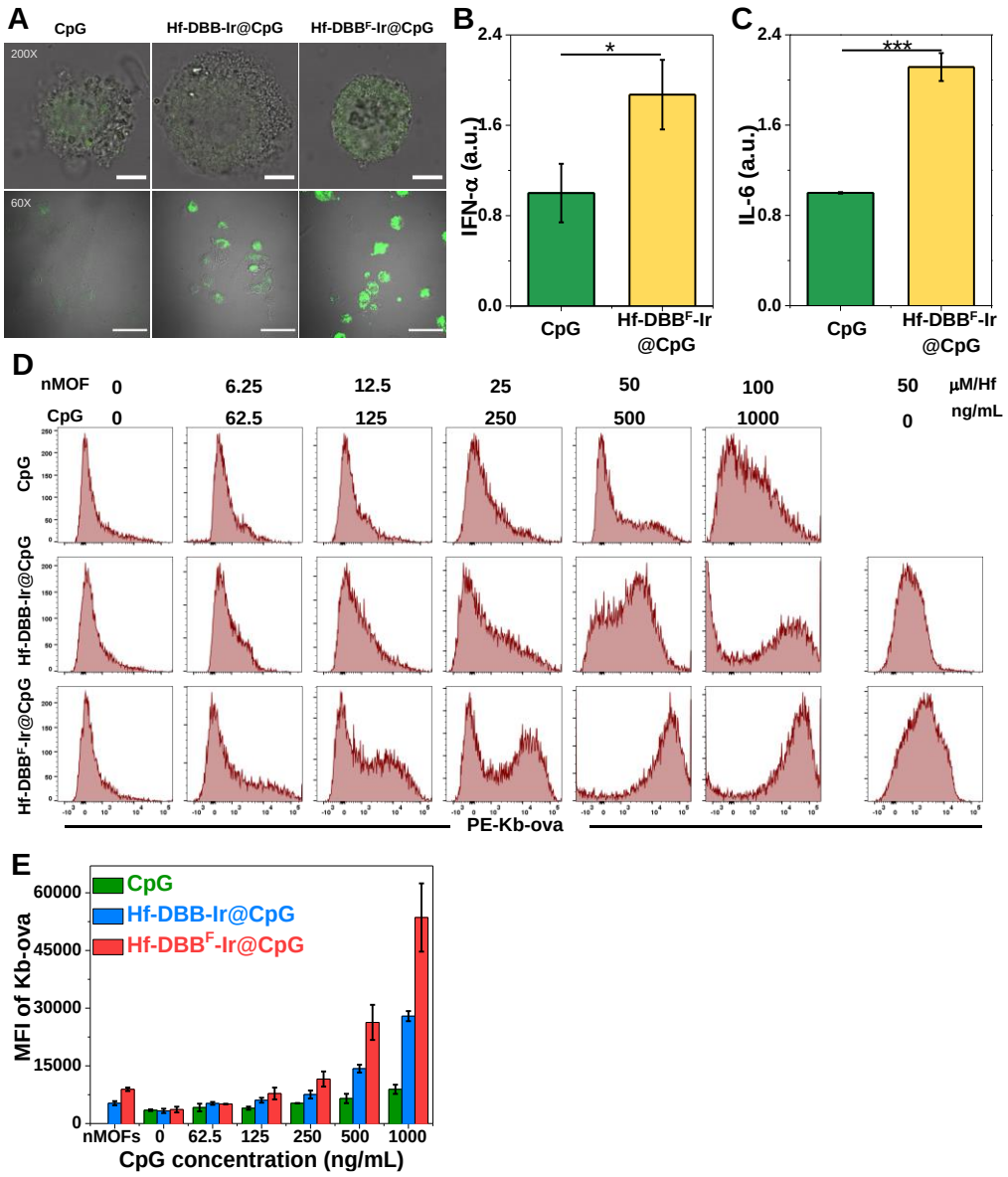

Fig. S5. Delivery of PAMPs and DC maturation. (**A**) DCs co-cultured with free CpG, Hf-DBB-Ir@CpG, or Hf-DBB^{F}-Ir@CpG for the observation of FITC-labelled CpG under CLSM. Top: magnification of 200-fold. Scale bar = 5 μm. Bottom: magnification of 60-fold. Scale bar = 50 μm. IFN-α (**B**) and IL-6 (**C**) expression levels quantified by qPCR, n=3. The Glyceraldehyde-3-phosphate dehydrogenase (GAPDH) was used as a housekeeping gene for comparison of gene expression. DCs were co-cultured with MC38-ova cells pre-treated with free CpG, Hf-DBB-Ir@CpG, or Hf-DBB^{F}-Ir@CpG plus X-ray irradiation at a dose of 2 Gy at a 1:3 ratio. (**D**) Representative figures represent CpG concentration-dependent Kb-ova expression on DCs. (**E**) Quantitative analysis of expression level of Kb-ova of DCs, n=3. Data are expressed as means ± s.d. (n = 3). *P < 0.05 and ***P < 0.001 by t-test.

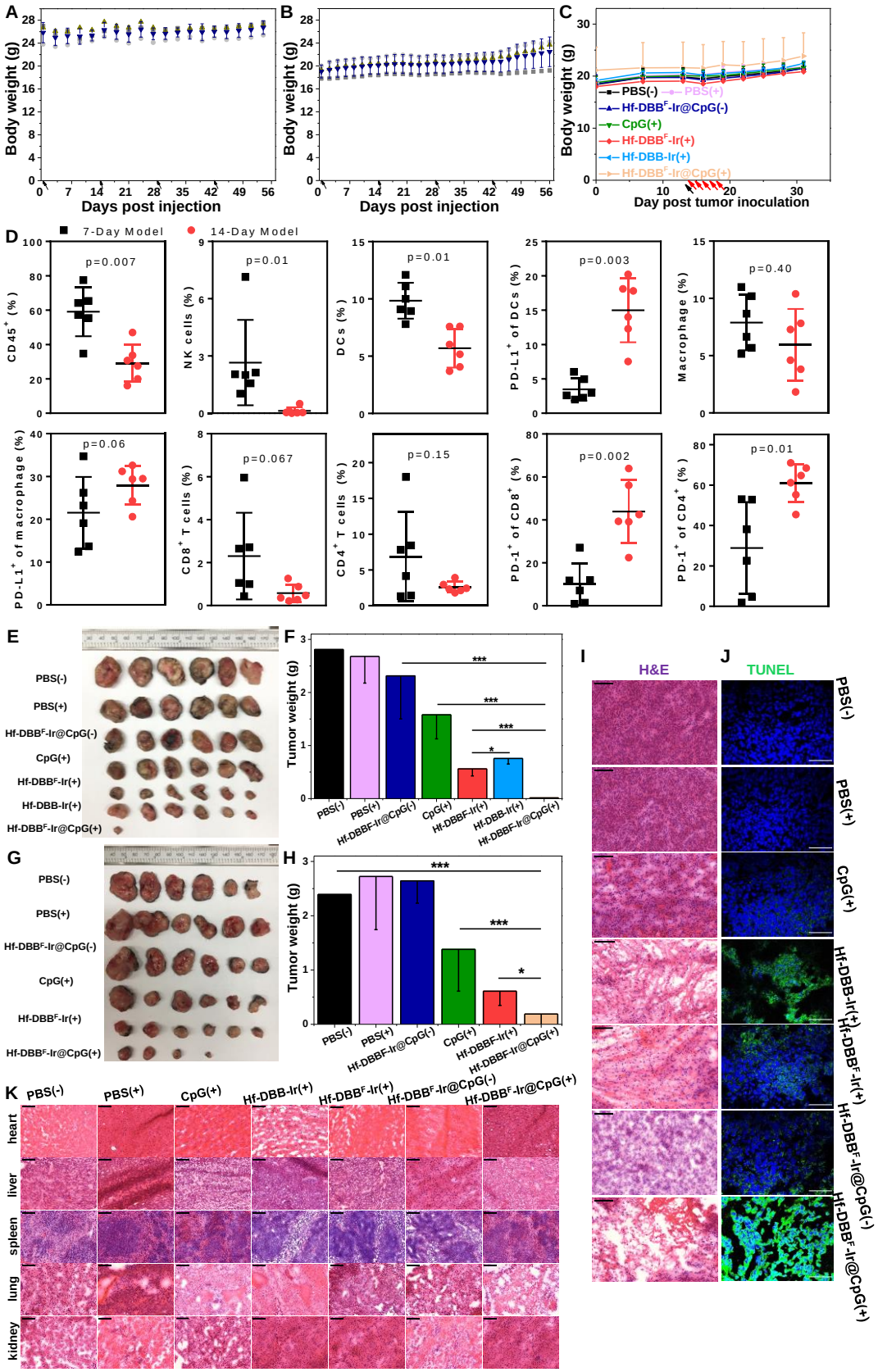

Fig. S6. *In vivo* toxicity and efficacy. Body weights of C57BL/6 mice were monitored after receiving DBB^F-Ir at a dose of 2 μmol biweekly with a total of four injections (**A**) or Hf-DBB^F-Ir at a dose of 2 μmol based on Hf biweekly with a total of four injections (**B**), n=3. Black arrows

refer to the times of injections. MC38-bearing C57BL/6 mice were treated with PBS(-), PBS(+), Hf-DBB^{F}-Ir@CpG(-), CpG(+), Hf-DBB^{F}-Ir(+), Hf-DBB-Ir(+), and Hf-DBB^{F}-Ir@CpG(+), n=6. (**C**) Body weights after tumor inoculation of MC38-bearing C57BL/6 mice. (**D**) Immune analyses of tumor microenvironment for 7-day and 14-day MC38 tumor models of 100~150 mm^3 in sizes, n=6. Photo (**E**) and weights (**F**) of excised tumors of MC38-bearing mice. Panc02-bearing C57BL/6 mice were treated with PBS(-), PBS(+), Hf-DBB^{F}-Ir@CpG(-), CpG(+), Hf-DBB^{F}-Ir(+), and Hf-DBB^{F}-Ir@CpG(+), n=6. Photo (**G**) and weights (**H**) of excised tumors of Panc02-bearing C57BL/6 mice. H&E staining (**I**) and TUNEL assay (**J**) of excised tumors of MC38-bearing C57BL/6 mice. From top to bottom: PBS(-), PBS(+), CpG(+), Hf-DBB^{F}-Ir(+), Hf-DBB-Ir(+)，Hf-DBB^{F}-Ir@CpG(-), and Hf-DBB^{F}-Ir@CpG(+). (**K**) Representative histology of frozen sections of major organs of MC38-bearing C57BL/6 mice. Scale bar = 100 μm. Data are expressed as means ± s.d. *P < 0.05 and ***P < 0.001 by t-test. Photo Credit: Kaiyuan Ni, the University of Chicago.

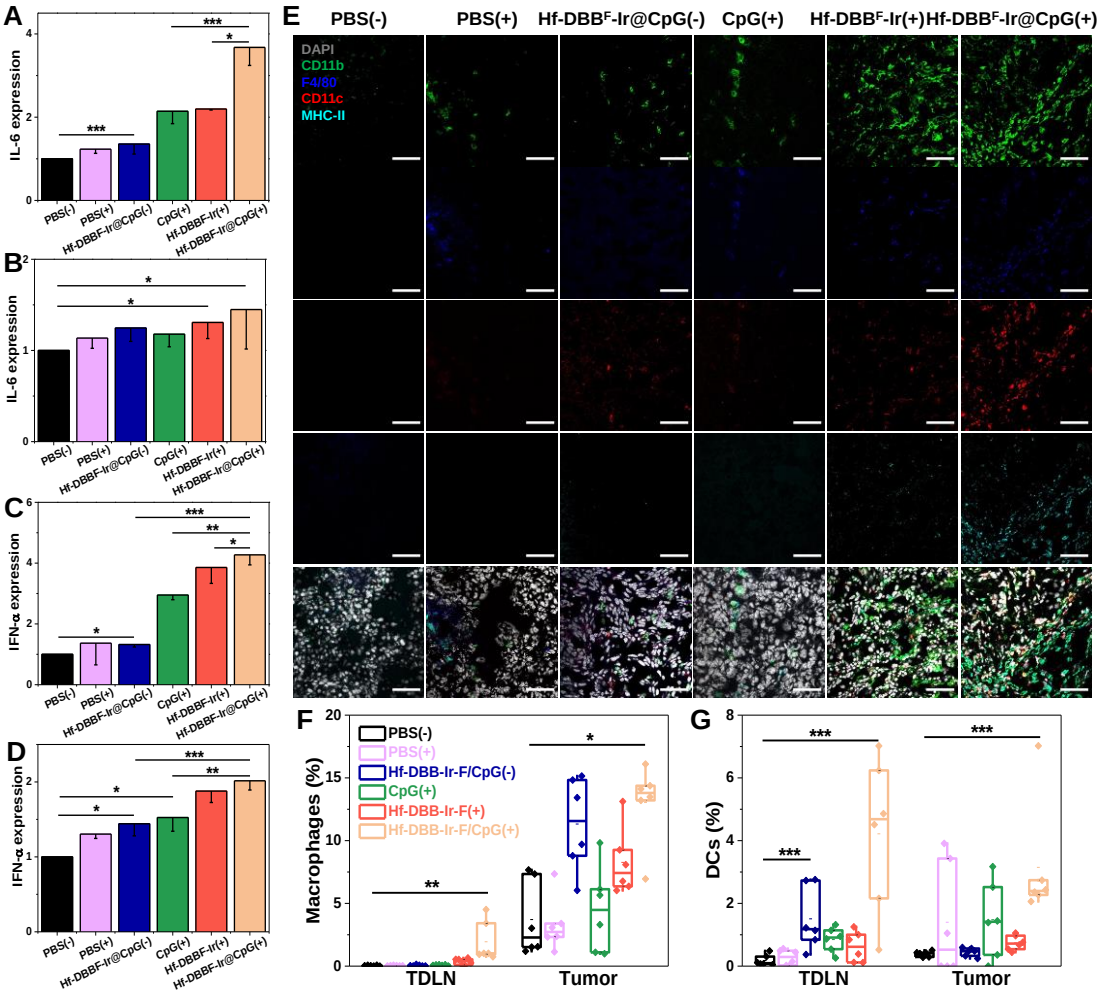

Fig. S7. *In vivo* APC maturation. MC38 tumors-bearing mice were treated with PBS(-), PBS(+), Hf-DBB^{F}-Ir@CpG(-), CpG(+), Hf-DBB^{F}-Ir(+), and Hf-DBB^{F}-Ir@CpG(+). IL-6 (**A**, **B**) or IFN-α (**C**, **D**) expression level of tumors (**A**, **C**) or tumor-draining lymph nodes (**B**, **D**) quantified by qPCR, n=4. GAPDH was used as a housekeeping gene for comparison of gene expression. (**E**) Representative CLSM images of tumor-infiltrating APCs. Grey, green, blue, red and cyan fluorescence indicate nucleus, CD11b, F4/80, CD11c and MHC-II, respectively. Scale bar = 100 μm. Percentages of macrophages (**F**), or DCs (**G**) with respect to the total cells in tumor-draining lymph nodes or tumors excised from MC38-ova tumor-bearing mice 6 days after the first irradiation treatment, n=6. Data are expressed as means ± s.d., *P < 0.05, **P < 0.01, and ***P < 0.001 by t-test. Central lines, bounds of box and whiskers represent mean values, 25% to 75% of the range of data and 1.5 fold of interquartile range away from outliers, respectively.

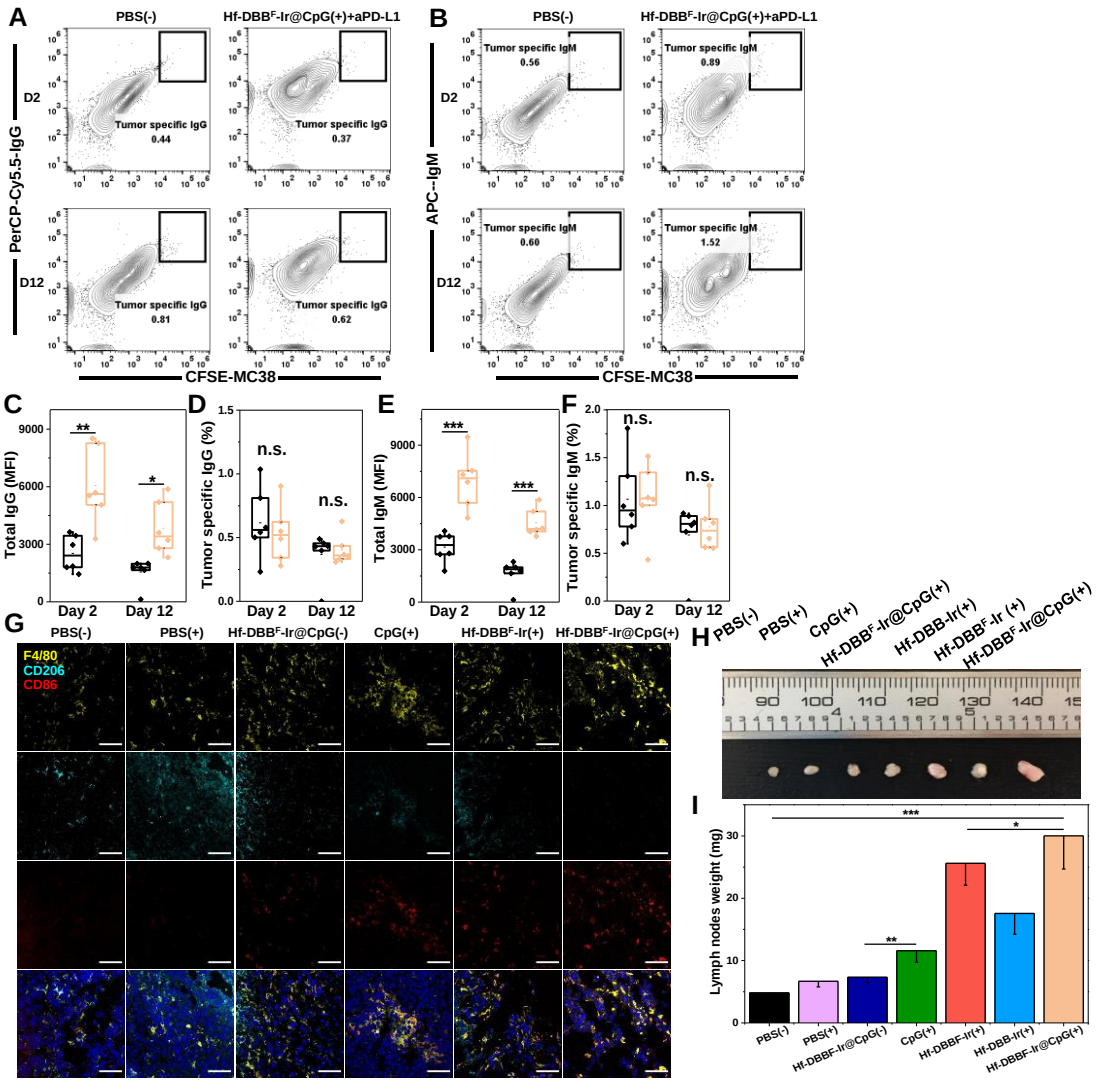

Fig. S8. Humoral immunity, macrophage repolarization and T cell expansion. MC38-bearing C57BL/6 mice were treated with PBS(-), PBS(+), Hf-DBB^F-Ir@CpG(-), CpG(+), Hf-DBB^F-Ir(+), Hf-DBB-Ir(+), and Hf-DBB^F-Ir@CpG(+). Day 2 or 12 post first irradiation, mice plasma were drawn and co-cultured with CFSE-labelled MC38 cells. Tumor-specific IgG (**A**, IgG$^+$CFSE$^+$) and IgM (**B**, IgM $^+$CFSE$^+$) were detected with flow cytometry. Quantification of total IgG (**C**), tumor-specific IgG (**D**), total IgM (**E**), and tumor-specific IgM (**F**), n=6. (**G**) Representative CLSM images for macrophage repolarization. Blue, yellow, cyan, and red fluorescence indicate nucleus, F4/80, CD206 and CD86, respectively. Scale bar = 100 μm. Photo (**H**) and weights (**I**) of excised tumor-draining lymph nodes, n=6. *P < 0.05, **P < 0.01, and ***P < 0.001 by t-test. Data are expressed as means ± s.d. Central lines, bounds of box and whiskers represent mean values, 25% to 75% of the range of data and 1.5 fold of interquartile range away from outliers, respectively. Photo Credit: Kaiyuan Ni, the University of Chicago.

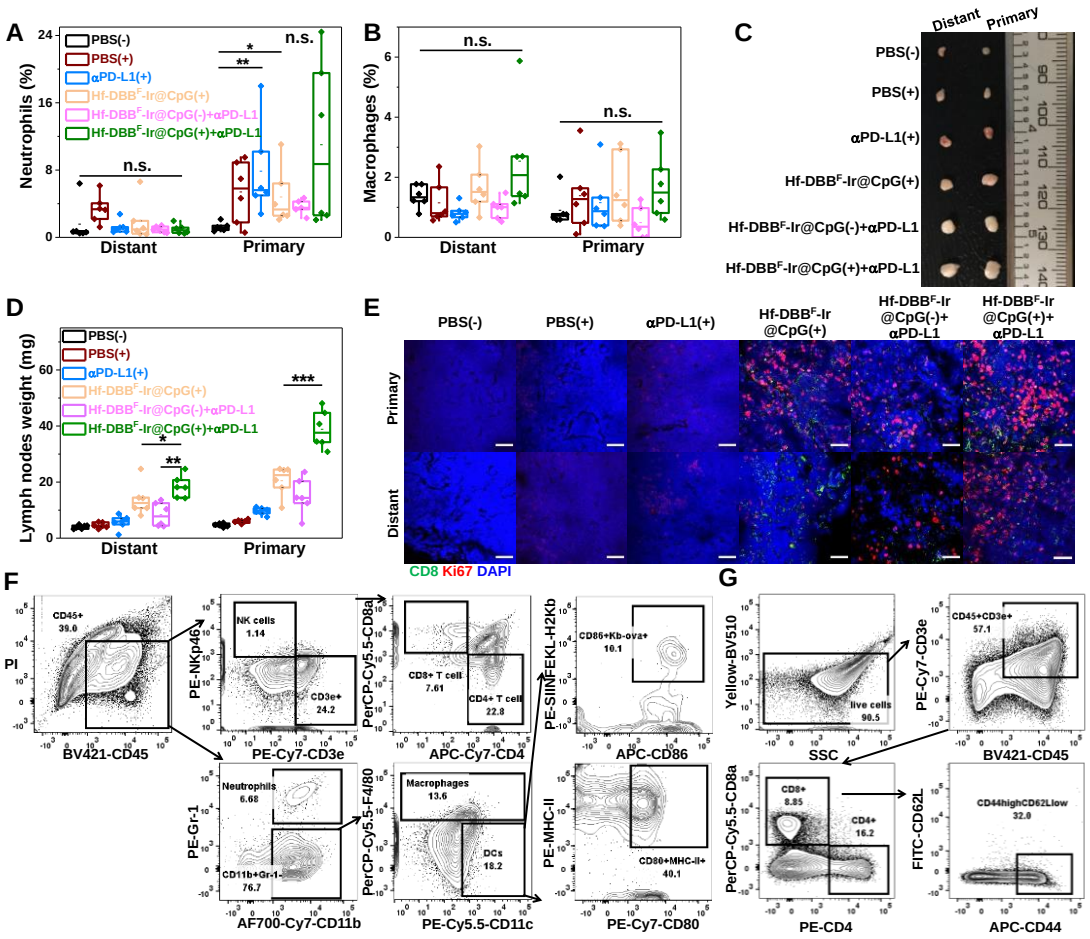

Fig. S9. Immune analysis on bilateral models. MC38-tumor bearing mice were treated with PBS(-), PBS(+), αPD-L1(+), Hf-DBB^{F}-Ir@CpG(+), Hf-DBB^{F}-Ir@CpG+αPD-L1(-), and Hf-DBB^{F}-Ir@CpG+αPD-L1(+). Percentages of neutrophils (**A**), or macrophages (**B**) with respect to the total cells infiltrated into tumors excised from bilateral MC38 tumor-bearing mice 10 days after the first irradiation treatment, n=6. Photo (**C**) and weights (**D**) of excised tumor-draining lymph nodes of mice, n=6. (**E**) Representative immunofluorescence imaging of excised tumor-draining lymph nodes of MC38-bearing C57BL/6 mice for detecting T cell expansion. Blue, green, and red fluorescence indicate nucleus, CD8α and Ki67, respectively. Scale bar = 100 μm. Data are expressed as means ± s.d. *P < 0.05, **P < 0.01, and ***P < 0.001 by t-test. (**F**) Representative gating strategies for CD45^{+} cells, NK cells, CD4^{+} T cells, CD8^{+} T cells, neutrophils, macrophages, dendritic cells, SIINFEKL-H_2Kb^{+} cells and CD80^{+} MHC-II^{+} cells profiled from tumor and lymph nodes. (**G**) Representative gating strategies for CD44^{high}CD62^{low} cells profiled from spleen. Photo Credit: Kaiyuan Ni, the University of Chicago.

Table S1. TGIs of MC38 and Panc02 tumor models after treatments.

TGI (%)	MC38	Panc02
PBS(+)	4.8	0.9
CpG(+)	34.8	54.8
Hf-DBB-Ir(+)	64.7	-
Hf-DBB^{F}-Ir(+)	81.9	69.4
Hf-DBB^{F}-Ir/CpG(-)	11.3	24.1
Hf-DBB^{F}-Ir/CpG(+)	99.6	89.1